Adaptive Antenna Control System for RFID Reader

P. Salonen, M. Keskilammi, L. Sydänheimo
Institute of Electronics
Tampere University of Technology
P.O. Box 692, FIN-33101 Tampere
FINLAND

Abstract: - Spatial filtering using adaptive or smart antennas has emerged as a promising technique to improve the performance of cellular mobile systems. Due to the digital nature of the control of spatial filtering a quantization error is readily present. This is due to the fact that weights and phase information is provided with the aid of finite wordlength processors. This paper presents the development of a five-element digital beam-forming antenna for RFID (radio frequency identification) reader operating on 2.4 GHz ISM-band. The paper presents detailed description of the operation of beam-form control including the analysis of 4-bit phase shifters. In addition, the result will show that the quantization error, even if it small, can degrade the pattern so dramatically making it unacceptable. However, we will show that with as low number of control bits as four the desired radiation characteristics can be achieved.

Key-Words: - Adaptive Antennas, Phase Shifter, Quantization Noise, Performance Analysis, RFID

1 Introduction

The development of radio frequency identification systems plays a significant role in the progress of rapidly expanding wireless applications. As part of the general identification procedure, radio frequency identification (RFID) is also an essential field of research in the modern industrial automation [1]. Radio frequency identification is used in all areas of automatic data capture allowing contactless identification of objects using radio frequencies. RFID technology plays an important role in controlling, detecting and tracking items and moving information efficiently with an item along the intelligent supply chain [2] – [3].

The RFID system generally consists of two basic components: the transponder and the reader. The transponder, or tag, is the data carrying device located on the object being identified – the paper reel. The reader can be a read or a read/write device that uses an antenna to send a radio frequency electromagnetic field to the tag. Both power and data can be sent. Once the tag is powered it will either send its stored data or be updated with new data depending on the wishes of the user.

This paper presents the development of a digital beam-forming antenna for 2.45 GHz RFID reader. The digital beam-forming antenna is used to allow multiple-target identification at once. This will improve the transports and warehousing logistics making them more reliable and faster.

2 A Control Unit for DBF Antenna

The antenna array is composed of five patch antennas with a half wavelength separation. The RFID reader and its antenna array is attached to a clamp-truck which is used for paper reel transportation in a warehouse. The theory of adaptive antennas is based on antenna arrays in which the radiation pattern can be controlled electrically by defining the weights for feed current amplitudes and proper phase shift for each of them. The block diagram of such an adaptive antenna control network is shown in Fig. 1, in which we can see that the digitally controlled phase shifters and current amplitude weights play a significant role in digital beam forming. The amplitude weighting can be done with an amplifier of which gain can be adjusted digitally. In this case the amplifier has 16 states which corresponds 4-bit control. The digitally controlled phase shifters are composed of cascade

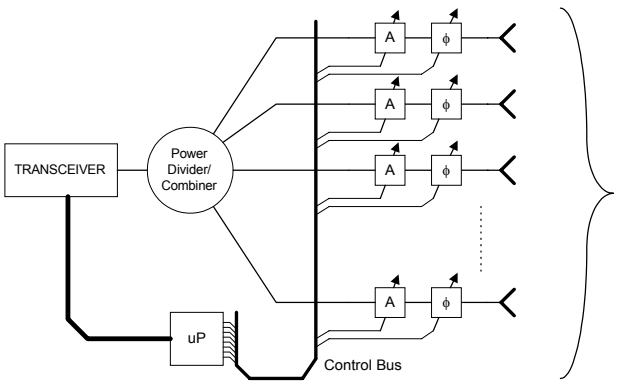

Fig. 1. Block diagram of the control network of digital beam-forming antenna.

connection of fixed-phase-shift phase shifters. These phase shifters can be made of 3dB branchline hybrid-couplers. The phase increment of 4-bit phase shifter equals 22.5°. The phase-shift error of less than ±1.5° over the designed 100 MHz frequency band centered at 2.45 GHz for the whole circuit can be achieved.

2.1 *pin*-Diode Phase Shifters

Phase shifter circuits can be divided broadly into two groups: the reflection type and the transmission type. The reflection-type phase shifter is basically a one-port device in which reflection of the microwave signal occurs at the termination of the transmission line. The magnitude of the reflection coefficient should ideally be unity in both switching states, and the phase shift is given by the change in the reflection coefficient. The transmission-type phase shifter is a two-port network in which the phase of the transmission coefficient through the network is altered by means of a switch while its magnitude remains nearly unity in both states [4].

There are three basic phase shifter circuits that use *pin*-diodes as the switching device: switched-line [4], loaded-line [5] – [6], and hybrid-coupled circuits [7] – [8]. The first two are transmission-type phase shifters, whereas the last is a reflection-type phase shifter. The switched-line phase shifter can be used for large phase shifts, i.e., 180° [4]. However, resonance may occur if the longer line is comparable with λ/2 or its multiples. This configuration needs 4 diodes per phase bit with an insertion loss of 1.5dB. The loaded-line phase shifter is suitable for small phase shifts of less than 45° [4] – [5]; the circuit needs two diodes, and the insertion loss can be made less than 1dB with 10% bandwidth. With hybrid-coupled phase shifters, all phase shifts can be realized [8] – [9] with 18% bandwidth in which the insertion loss is less than 1dB.

These results show that to obtain a 4-bit phase shifter, an insertion loss of 4 – 5 dB should be expected and taken into account in designing amplifiers that feed the antenna elements in the array. In addition, the phase error caused by each phase bit is ±2° in 10% bandwidth with all the phase shifter circuits [6], [10]. Thus, a typical phase deviation of 8° within the band in the four-bit phase shifter should be expected.

2.2 Analysis of Hybrid-Coupled Phase Shifter

The hybrid coupled phase shifter makes use of a 3dB, 90° hybrid coupler with two of its ports terminated in symmetric phase-controllable reflective networks. Short-circuited transmission line is used as reflective network of which length is controlled by a *pin*-diode. The coupler divides the input signal equally between the two output ports (ports 3 and 4) but with phase difference of 90°, Fig. 2. Signals reflected back from the two symmetric terminations add up at port 2 and no signal returns to port 1. The hybrid coupler offers a match transmission behavior for the phase shifter bit. According to [7] and [9] hybrid coupled phase shifters are slightly superior to others due to a lower number of diodes per phase bit, smaller size, higher power handling capacity and the ability to obtain any desired phase bit.

A branchline hybrid can be analyzed by using even-odd mode analysis method in which the hybrid is divided into transmission line sections. These sections consist of open-circuited shunt-stubs (even-mode) and short-circuited stubs (odd-mode) and λ/4 transmission line in between. These sections are cascaded by using transmission-parameters (*ABCD*). Resulted scattering-parameters (*S-parameters*) are after *ABCD*-to-*S*-parameter transformation: $S_{11} = (S_{11e} + S_{11o})/2$, $S_{12} = (S_{11e} - S_{11o})/2$, $S_{13} = (S_{14e} - S_{14o})/2$, $S_{14} = (S_{14e}+S_{14o})/2$, in which

$$S_{11e} = -\frac{j}{\Delta_e}\left[2p\cos\theta - \frac{p^2}{\sqrt{2}}\sin\theta + \frac{\sin\theta}{\sqrt{2}}\right] \quad (1)$$

$$S_{11o} = -\frac{j}{\Delta_o}\left[-\frac{2\cos\theta}{p} - \frac{\sin\theta}{\sqrt{2}p^2} + \frac{\sin\theta}{\sqrt{2}}\right] \quad (2)$$

$$S_{14e} = \frac{2}{\Delta_e} \quad (3)$$

$$S_{14o} = \frac{2}{\Delta_o} \quad (4)$$

$$\Delta_e = \left(2\cos\theta - \sqrt{2}p\sin\theta\right) + j\left(2p\cos\theta - \frac{p^2}{\sqrt{2}}\sin\theta + \frac{3}{\sqrt{2}}\sin\theta\right) \quad (5)$$

$$\Delta_o = \left(2\cos\theta + \frac{\sqrt{2}\sin\theta}{p}\right) + j\left(-\frac{2\cos\theta}{p} - \frac{\sin\theta}{\sqrt{2}p^2} + \frac{3}{\sqrt{2}}\sin\theta\right) \quad (6)$$

$$p = \tan\frac{\theta}{2}, \quad \theta = \frac{2\pi}{\lambda}l = \frac{\pi}{2}\frac{\lambda_0}{\lambda}$$

where λ_0 is the wavelength at the design frequency. The remaining *S*-parameters can be found by transposition because the hybrid is symmetric between all of its ports.

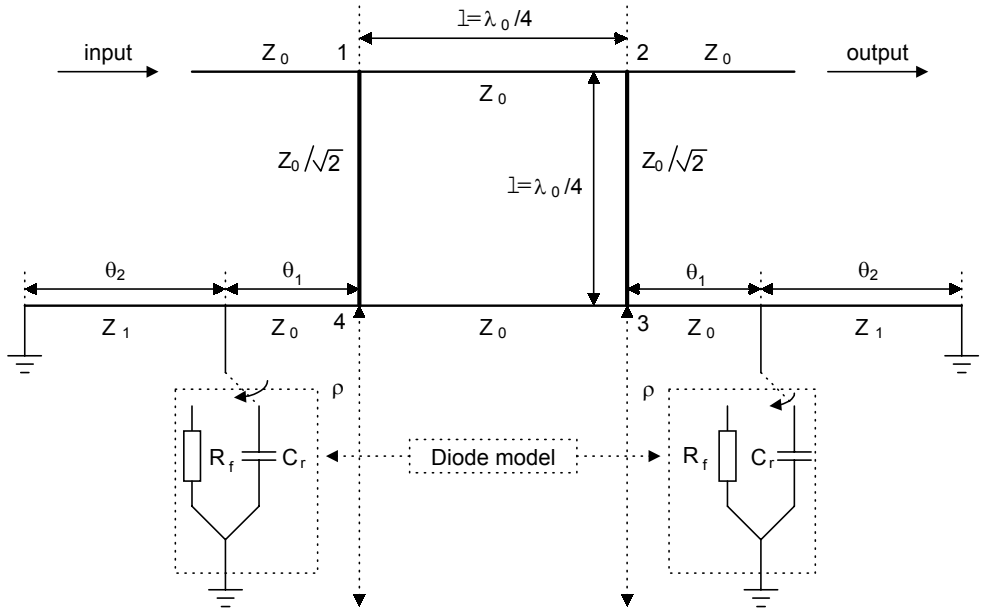

Fig. 2. Branchline hybrid-coupled phase shifter with reflective network. Equivalent diode model used to find reflection coefficient of the termination is also shown. Bias network is omitted.

The reflective network consists of a short-circuited transmission line and shunt *pin*-diode, Fig. 2. Different impedance values for transmission line sections θ_1 and θ_2 are allowed to increase the degree of freedom in designing. For a chip diode the diode equivalent circuit consists of small resistance R_f which is a function of bias current and capacitance C_r which is a function of bias voltage for forward and reverse bias conditions, respectively [4]. The reflection coefficient ρ can be found by combining the effect of short-circuited transmission line and the *pin*-diode parameters in different bias conditions as a function of lengths of transmission line sections θ_1, θ_2, frequency f, and diode parameters.

2.3 Performance of the Digitally Controlled Phase Shifter

The reflection coefficients of the reflective network are used in finding the total reflection and transmission coefficients of hybrid coupled phase shifter. In the analysis it is assumed that hybrid is symmetric despite of the addition of reflective networks. For a unit input fed to port 1, the signals S_{13} and S_{14} emerging out of ports 3 and 4 are reflected back. The reflected signals ρS_{13} and ρS_{14} form inputs to ports 3 and 4, respectively. These signals are distributed between four ports. Signals emerging from ports 1 and 2 are absorbed as they are match terminated, but the signals emerging from ports 3 and 4 are reflected back again by the terminations. Considering multiple reflections the overall transmission coefficient T_{21} from port 1 to port 2 and the overall reflection coefficient R_{11} at port 1 can be found as [4]

$$T_{21} = S_{12} + \rho\begin{bmatrix} S_{13} & S_{14} \end{bmatrix}\begin{bmatrix} 1-\rho S_{11} & -\rho S_{12} \\ -\rho S_{12} & 1-\rho S_{11} \end{bmatrix}^{-1}\begin{bmatrix} S_{14} \\ S_{13} \end{bmatrix} \quad (7)$$

$$R_{11} = S_{11} + \rho\begin{bmatrix} S_{14} & S_{13} \end{bmatrix}\begin{bmatrix} 1-\rho S_{11} & -\rho S_{12} \\ -\rho S_{12} & 1-\rho S_{11} \end{bmatrix}^{-1}\begin{bmatrix} S_{14} \\ S_{13} \end{bmatrix} \quad (8)$$

These are the design equations for any hybrid coupled phase shifter using phase controllable reflective networks. Of this two-port system *S*-parameters can then be transformed to *ABCD*-parameters to find the total effect of 4-bit phase shifter on differential phase of any bit combination and the attenuation caused by the different reflective networks. This analysis does not take into account the material losses, only the losses due to matching the transmission line and diodes.

Fig. 3. shows that varying the length of short-circuited transmission line and its impedance the desired phase shift with phase shift error less than 1° can be obtained over desired bandwidth. However, in this example all impedance values are 50Ω. It was observed that the length of θ_2 controls the differential phase shift nearly linearly.

The phase error of the 4-bit phase shifter stays below ±1° for any bit combination. The increased error is due to the combination of four different phase shifters with their own phase shift error. *VSWR* is less

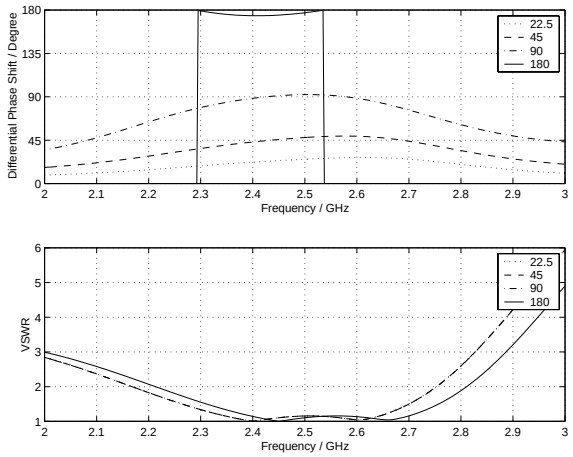

Fig. 3. Phase difference and *VSWR* as a function of frequency for 180°, 90°, 45°, 22.5° branchline hybrid-coupled phase shifters. $\theta_1 = 63°$ for all phase shifters, $\theta_2 = [77.4°, 37{,}8°, 19.8°, 10.8°]$, impedance values for θ_1 and θ_2 are 50Ω for 180°, 90°, 45°, 22.5° hybrids, respectively.

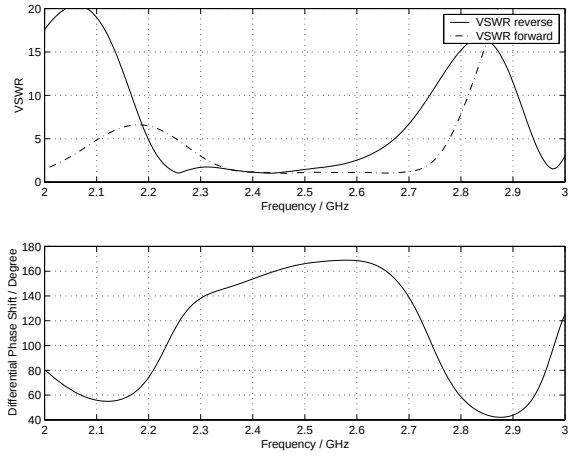

Fig. 4. Phase difference and *VSWR* as a function of frequency for a 4-bit branchline hybrid coupled phase shifter at differential phase shift of 157.5°. *VSWR* reverse and *VSWR* forward stands for the diode's reverse and forward biased conditions, respectively.

than 1.5 for any bit combination at operating band (2.4GHz – 2.5GHz). Fig. 4. shows an example of 157.5° phase difference in which 22.5°, 45° and 90° hybrids are reverse biased and 180° hybrid is forward biased. This shows that in theory a good quality small low-cost 4-bit branchline hybrid coupled phase shifter using *pin*-diodes can be designed.

Fig. 5. shows the measured and theoretical results for 45° hybrid-coupled phase shifter. Due to the hand-made prototype the differences from theoretical results could be expected. However, these results

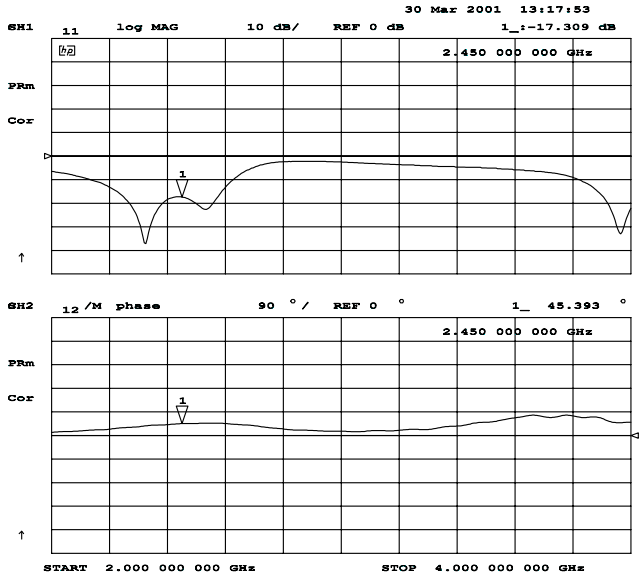

Fig. 5. Measured return loss and differential phase shift for 45° hybrid coupled phase shifter.

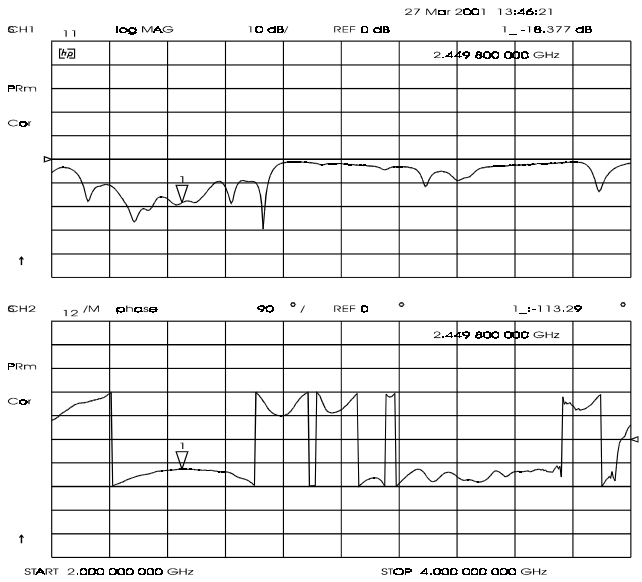

Fig. 6. Measured return loss and differential phase shift for the 4-bit hybrid-coupled phase shifter. Graphs are shown for which differential phase shift of -112.5° is selected.

show that good agreement with theory were observed.

In fig. 6. measured results are shown for the 4-bit hybrid coupled phase shifter. Phase shifters are cascaded in descending order in which 180° phase shifter is first followed by 90° and so on. Theoretical results were calculated with the same order. All phase shifters were hand-made and similar error sources are encountered as discussed previously.

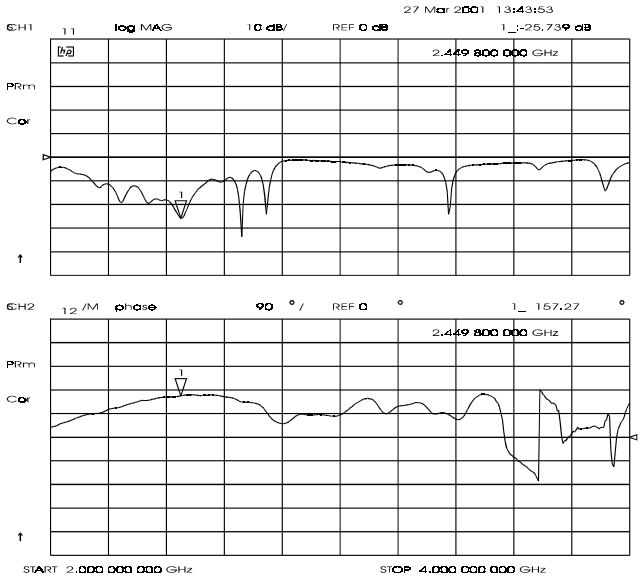

Fig. 7. Measured return loss and differential phase shift for cascade 157.5° 4-bit hybrid coupled phase shifter.

Theoretical and measured results agree well over the desired frequency band. The agreement of the differential phase shift is exact at the designed point frequency, that is 2.45GHz. However, the return loss is high enough that the 4-bit hybrid coupled phase shifter operation agrees well with the desired bandwidth specifications. Similar results were observed with other differential phase shift values in which other example is for 157.5° differential phase shift, Fig. 7. For all phase shifts the insertion loss was less than 7dB. In theory the expected insertion loss was 6dB with lossless substrate.

3. Digital Beam-Forming and Coefficient Quantization

Spatial filtering using adaptive or smart antennas has emerged as a promising technique to improve the performance of cellular mobile systems. To achieve the ambitious requirements introduced for future wireless systems new intelligent or self-configured and highly efficient systems will most certainly be required. In the pursuit of schemes that will solve these problems attention has recently turned to spatial filtering using advanced antenna techniques: adaptive or smart antennas [11] – [12]. Filtering in the space domain can separate spectrally and temporally overlapping signals from multiple mobile units and hence the spatial dimension can be exploited as a hybrid multiple access technique complementing FDMA, TDMA and CDMA.

However, due to the digital nature of the control of spatial filtering a quantization error is readily present. This is due to the fact that weights and phase information is provided with finite wordlength processors. Various radiation pattern synthesis algorithms are usually very accurate to several places of decimals. To implement the radiation pattern, the feed current coefficients in an array factor must be represented by a fixed number of bits and very often this is determined by the wordlength of the processor used. The effect of coefficient errors is to cause the radiation pattern to deviate from the desired pattern. This deviation in the extreme case will mean that the specifications are no longer met.

Despite of the previously described limitations adaptive antennas offer a unique solution to establish a radio link between RFID devices. The weights of current amplitude are presented with four bits. Similarly the feed current phase is presented with four bits. This means that study of subarray performance is not required [13] and the number of bits controlling the weights and phase of the feed-current can be limited to four. Due to quantization errors a trade off between minimum sidelobe level and half power beam width is to be made. This is due to the fact that e.g. with Chebychev current distribution of given beam width a minimum sidelobe level is achieved and typically this distribution is not achieved with reduced number of bits.

If an array factor of at least –30dB side lobe level is needed for a five-element antenna array, the effect of quantization on the initial radiation pattern fails to give that value. The initial design is based on the Dolph-Chebyshev synthesis method. This method gives the current amplitudes as (0.318 0.768 1 0.768 0.318) and the resulting pattern is shown in Fig. 8. This radiation pattern has the maximum sidelobe level of –30dB, as expected. However, after quantization (current amplitudes: 0.3125 0.8125 1 0.8125 0.3125) the sidelobe level is increased 4dB (the sidelobe level is –26dB) and thus this does not meet the specified value anymore. By finding a combination from the set of 4-bit coefficients such that the specified sidelobe level is obtained, the resultant coefficients will be (0.25 0.75 1 0.75 0.25). With these coefficients the maximum side lobe level is –33.6dB, which meets the specified value. However, the half-power beam-width is increased approximately only 1° compared with the initial Dolph-Chebychev current distribution. The results are summarized in Fig. 8.

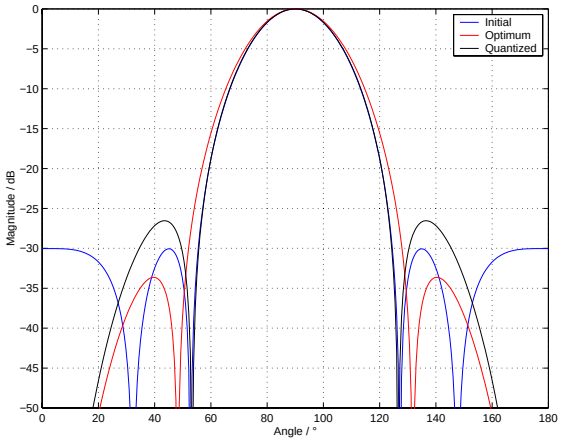

Fig. 8. Decrease in sidelobe level due to coefficient quantization error.

4. Conclusions

In this paper we have analyzed the performance of a five-element adaptive antenna for RFID reader at 2.45 GHz. The main emphasis was to develop accurate 4-bit *pin*-diode phase shifters. In addition the effect of coefficient quantization on the radiation pattern was analyzed. First, all required phase shifters were designed separately and then combined to form 4-bit phase shifter circuit. Both were theoretically analyzed and the analyzed results were verified in practice with very good agreement. In the desired frequency band *VSWR* was less than 1.5 for all phase shifters separately and together. The insertion loss was not more than 7 dB for the cascaded phase shifter.

In addition it was shown that the quantization error, even if it small, can degrade the pattern so dramatically making it unacceptable. In worst case this means that the desired signal can not be received. However, by optimizing the error the desired pattern can be achieved. This means that the error in a single current amplitude might be larger compared with the initial quantization error but the total error to desired radiation pattern is minimized. In addition this shows very well that with as low number of control bits as four most of the desired radiation patterns can be achieved or at least an acceptable compromise is obtainable. This study clearly shows that for small arrays the radiation pattern degradation due to quantization becomes more important in order to achieve the desired radiation characteristics.

References:

[1] Finkenzeller, K., *RFID Handbook, Radio-Frequency Identification Fundamentals and Identification*, John Wiley & Sons Inc., 1999.

[2] Keskilammi, M., Sydänheimo, L., Salonen, P., Kivikoski, M., Controlling Paper Reel Handling and Transportation with Intelligent RFID System, *Proceedings of the IASTED International Conference, Modelling, Identification, and Control*, pp. 953 – 958, 2001.

[3] Keskilammi, M., Salonen, M., Sydänheimo, L., Kivikoski, M., Antenna Demands for RFID Interface in Paper Reel Supply Chain, *Proceedings of the IASTED International Conference, Robotics & Manufacturing*, pp. 99 – 104, 2001.

[4] Koul, S. K., Bhat, B., *Microwave and Millimeter Wave Phase Shifters*, Vol. II, Artech House, 1991.

[5] Bahl, I. J., Gupta, K. C., Design of Loaded-Line p-I-n Diode Phase Shifter, *IEEE Trans. MTT*, Vol. 28, No. 3, pp. 219 – 224, March 1980.

[6] Atwater, H. A., Circuit Design of the Loaded-Line Phase Shifter, *IEEE Trans. MTT*, Vol. 33, No. 7, pp. 626 – 634, July 1985.

[7] Kori, M. H., Mahapatra, S., Integral Analysis of Hybrid Coupled Semiconductor Phase Shifters, *IEE Proc*, Vol. 134, Pt. H, No. 2, pp. 156 – 162, April 1987.

[8] Karmakar, N. C., Bialkowski, M. E., An L-Band 90 Hybrid-Coupled Phase Shifter Using UHF Band p-I-n Diodes, *Microwave and Optical Technology Letters*, Vol. 21, No. 1, pp. 51 – 54, April 1999.

[9] Bialkowski, M. E, Karmakar, N. C, Design of Compact L-Band 180 Phase Shifters, *Microwave and Optical Technology Letters*, Vol. 22, No. 2, pp. 144 – 148, July 1999.

[10] Karmakar, N. C., Bialkowski, M. E., Low Cost Phase Shifters for L- Band Phased Array Antennas, *IEEE Intl. Symposium on Antennas and Propagation*, 1997 Digest, Volume: 4, 1997 pp. 2476 -2479 vol.4, 1997.

[11] Tsoulos, G. V., Smart Antennas for Mobile Communication Systems: Benefits and Challenges, Electronics and Communication Engineering Journal, pp. 84 – 94, Apr. 1999.

[12] Drabowitch, S., Papiernik, A., Griffiths, H., Encinas, J., Smith, B. L., *Modern Antennas*, Chapman & Hall, 1998.

[13] Hansen, R. C., Subarray Quantization Lobe Decollimation, IEEE Trans. Antennas and Propagat. Vol. 47, No. 8, pp. 1237 – 1239, Aug. 1999.